

Research Article

Experimental Study on Seismic Performance of Prefabricated Frame Column Joints with a High Axial Compression Ratio

Y. L. Wang ¹, X. Y. Wu ¹, and B. B. Li ²

¹Department of Civil Engineering, Tianjin Chengjian University, Tianjin 300384, China

²China Railway Construction Group Co., Ltd., Beijing 100040, China

Correspondence should be addressed to X. Y. Wu; wuxy0614@163.com

Received 18 April 2022; Revised 13 June 2022; Accepted 8 July 2022; Published 5 August 2022

Academic Editor: Roberto Nascimbene

Copyright © 2022 Y. L. Wang et al. This is an open access article distributed under the Creative Commons Attribution License, which permits unrestricted use, distribution, and reproduction in any medium, provided the original work is properly cited.

A new type of an assembled monolithic concrete column encased by partial outsourcing steel was proposed, and the seismic performance was proposed. To study the seismic performance such as failure mode, hysteretic behavior, deformation, ductility of the specimen, and the influence of the outsourcing steel pipe on the mechanical performance of the specimens, the comparative tests of four full-scale specimens under low cyclic reciprocating load under a high axial compression ratio were carried out. The test results show that the monolithic column assembled with outsourced steel has better overall performance, and the failure of the specimen is the large eccentric compression failure with good ductility. The hysteresis and skeleton curves of the assembled columns are similar to the cast-in-site concrete column under the same conditions, which have a good ductility and energy dissipation capacity. It was established that increasing the thickness of the outer steel plate does not significantly improve the mechanical performance of the component when the load-bearing capacity of members satisfies the design requirements. The research results can provide a reference for theoretical research and practical engineering applications of assembled monolithic concrete column connections.

1. Introduction

As a kind of building structure with obvious advantages, the prefabricated concrete structure is bound to become one of the development directions of building industrialization in the future, and the main factor restricting the development of prefabricated concrete structures is the connection of joints. Columns are the main lateral force resisting component system of frame structures and frame-shear structures, so it is essential to study the seismic performance of columns and the connection of column joints for assembled monolithic structures.

In recent years, scholars have conducted a lot of research studies on the connection of column joints. Shi [1] improved the formulae of the compressive strength of the assembled steel tube-confined concrete column. Luo [2] improved the traditional tenon connection of precast monolithic RC frame columns. The experimental and analytical results of Haber [3] were used to support the discussion of design

considerations and an approximate method for calculating the displacement ductility of precast columns with grouted sleeve connections and shifted plastic hinging. Wei [4] completed low cyclic loading test research studies on the new prefabricated column-to-column connection joint, which consists of three kinds of connected devices, including unbonded prestressed tendons, brass friction energy dissipators, and angle steel. Wei [5] discussed a test carried out on the prefabricated concrete column joint reserved with wall panel slots and connected by angle steel and grouting sleeve, and the analysis results of the finite element were compared with the experimental results to verify the accuracy of the theoretical analysis. Hu [6] presented a precast concrete-based dry mechanical joint for fully restrained moment connections, and the experiments and the finite element analysis verify that the joints have sufficient stiffness and strength and show a similar structural behavior to traditional columns. Liu [7] introduces two types of bolted splice joints for square steel tubes with a smaller tube as a

splice component inside. Axial-compression and eccentric-compression tests were conducted on eight specimens to obtain the load transfer mechanism, load carrying capacity, and damage behavior. Ding et al. [8, 9] conducted relevant experimental research on the seismic performance of concrete-filled steel tubular columns under the condition of the high axial compression ratio. Liang [10] completed a test under cyclic low cycle load on a new type of fully assembled column-column dry concrete frame column joints. Lv [11] presented a new type of the assembled column-column connection joint that is proposed in the study and studied the force failure process and shape of the assembled column under different stress conditions and the influence of the parameters on the partial pressure bearing capacity and the strain of the steel bar. Liu [12] presented a new type of a precast concrete column-column joint and its corresponding column base joint with a steel jacket for confining the concrete core and the bolted flange plate and verified the reliability of the precast column by experiments. Li [13] completed a test under cyclic loading on 12 laminated reinforced concrete shear walls, the seismic performance was evaluated, and the influence of two different construction measures and construction technology on its performance is also studied. Tao [14] studied the influence of changing the internal structure of the outer steel plate on the bearing capacity of the SCFC column joint. Zheng [15] conducted a study on the seismic behavior of precast concrete column specimens before and after treatment of sleeve grouting defects. Wang [16] studied the seismic behavior of the new type of assembled special-shaped column joints by conducting quasi-static tests on two groups of special-shaped column joints. Gao [17] tested the full-scale test model of an assembled frame single tenon column joint with a wall panel slot. Lu [18] conducted the pseudo-static tests on six columns in order to validate the seismic performance of precast concrete members with steel sleeve connections and proposed some recommendations on practical seismic design pertinent to the precast concrete. The research by Lv [19] studied the seismic performance and replaceable performance of a new prefabricated composite column with replaceable components based on reinforced concrete-steel (RCS) hybrid frame structures and provides a new thought on the connection of assembled column joints.

In this paper, a new type of assembled monolithic concrete columns encased by partial outsourcing steel was proposed; that is, the column joint is connected through the outsourcing steel pipe welded by two “[” shaped steel, and the transverse bolt rod is set between the outsourcing steel pipe and the precast concrete column; the gap between the steel pipe and the column is filled by the grouting material with high strength to improve the mechanical performance of the connection. With the increase in building height and span, the vertical load borne by the lower load-bearing columns in reinforced concrete frame structures and frame-shear wall structures increases significantly, resulting in high axial compression ratio columns. Therefore, it is necessary to conduct experimental research on the seismic performance of high axial

compression ratio columns to ensure the safety of structures in earthquakes. Through the comparative test of four full-scale specimens with the above connection under horizontal cyclic loading with the high axial compression ratio, the failure mode, hysteresis curves, and skeleton curves are studied, and their seismic performance is analyzed.

2. Test Overview

2.1. Specimen Design. In this experiment, three full-scale-assembled monolithic concrete columns encased by partial outsourcing steel specimens and a full-scale monolithic cast-in-situ concrete column comparison specimen are designed, respectively, numbered as W01, W02, W03, and XJ-01. Among them, W01, W02, and W03 are assembled monolithic columns with a locally encased steel pipe (hereinafter referred to as assembled columns); XJ-01 is a monolithic cast-in-situ concrete column as the comparison component. In this test, all specimens are made of C40 concrete with an axial compression ratio of 0.6, and the shear-span ratio is 4.5. The structure of each specimen is detailed as follows.

The assembled column is connected by an upper column with a height of 1200 mm and a lower column with a height of 1500 mm (including the foundation beam). The calculated column height is 1900 mm, and the actual column height is 2100 mm. The upper column and the lower column are equipped with 8 HRB400 steel bars with a diameter of 22 mm, along the full length of the column with rectangular high-strength composite spiral stirrups, the high-strength spiral stirrups are high-frequency heat-treated steel bars with a diameter of 5 mm, with a spacing of 50 mm (the stirrup encryption zone is 30 mm), and the tensile strength of the stirrups is 1100 MPa. The connecting area of the upper and lower columns is provided with an outer steel pipe, which is welded by two identical “[” shaped steel made of tear plates, and the reserved gap between the outer steel pipe and the concrete column is 5–10 mm, which is bonded by a high-strength grouting material in the later stage. In addition, 8 transverse reinforcements are set in the connection area of the upper and lower columns, passing through the reserved holes of the concrete column along the horizontal force loading direction, and both ends are welded with the wrapped steel hoops. The height of W01 and W02 steel tubes is 1290 mm, and the outsourcing steel pipe restrained the column foot with a thickness of 5 mm (effective thickness is 3.8 mm) and 8 mm (effective thickness is 6.8 mm). The outsourcing steel pipe height of the specimen W03 is 850 mm, and the steel pipe is only set at the connecting area of the upper and lower columns according to the anchorage requirements, while the column foot is not restrained; the thickness of the steel plate is 5 mm. The specimen XJ01 is a cast-in-situ comparison column. The stirrup is equipped with a 5 mm diameter rectangular high-strength composite spiral hoop with a space of 50 mm, and the longitudinal reinforcement is equipped with 8 HRB400 steel bars with a diameter of 22 mm. The main parameters are shown in Tables 1–3, and the specimen structure is shown in Figure 1.

TABLE 1: Material properties of concrete.

Standard value of compressive strength of concrete cube ($f_{cu,k}$)	45.38 MPa
Standard value of axial compressive strength of concrete (f_{ck})	30.35 MPa
Elastic modulus of concrete (E_c)	3.38×10^4 N/mm ²

TABLE 2: Material properties of the steel plate pipe.

Specimens	Thickness of the tear plate (mm)	Actual thickness (mm)	Yield strength (MPa)	Ultimate strength (MPa)
W01	5	3.8	320	475
W02	8	6.8	290	405
W03	5	3.8	320	475

TABLE 3: Material properties of longitudinal reinforcement.

Diameter (mm)	Yield strength (MPa)	Tensile strength (MPa)	Elongation (%)	Yield ratio	Bending test
22	490	660	24	1.35	Flawless

2.2. Test Device and the Loading System. In this test, the pseudo-static test method is adopted to simulate the force and deformation characteristics of the structure or component in the seismic reciprocating vibration by applying the horizontal reciprocating cyclic load to the component, to obtain the inelastic load and deformation characteristics of the component. The loading device and specimens fixed on it are shown in Figure 2. Due to the low loading rate of the quasi-static test method and no inertial force during the test, the change rate of stress and strain caused by the loading rate has little effect on the test results and can be ignored [20].

The loading system of this test adopts the method of force and displacement mixed loading; that is, force control loading is adopted before the specimen yields. With each increase of 50 kN in the first cycle, each load level is 1 cycle. After yielding, the yield displacement Δy is used to control loadings, Δy , $2\Delta y$, and $3\Delta y$, . . . which were used as the cycle level for cyclic loading, 3 cycles for each level, and loading should be stopped until the load drops to 85% of the ultimate load [21, 22]. The loading system is shown in Figure 3.

3. Test Results and Analysis

3.1. Failure Modes of Specimens. There were four specimens in this test. In terms of the test process and failure characteristics, all specimens experienced three stages, crack-free work, jointed work, and failure. The failure of all specimens occurs at the maximum bending moment of the column base, presenting the expected bending failure state.

During the test, no out-of-plane deformation such as bulging, buckling, and cracking was observed in the outer steel tubes of specimens W01, W02, and W03. The measured strain of the wrapped steel plate is much less than the yield strain of the steel. On the tensile side of the column, there is a slight separation between the top and bottom of the steel pipe and the column due to the bending deformation of the column when the loading displacement is large, and the overall slip between the column and the steel pipe does not occur. No damage was found in the inspection of the welding point of the transverse reinforcement and the outsourced steel pipe at the end of the test.

For specimens W01, W02, and W03, the plastic hinge zone of specimens with a high axial compression ratio is very large. All below the joint seam of the assembled column are plastic hinge areas. After stripping the steel pipe of the test piece, it is found that the bonding grouting material between the steel pipe of the upper column and the lower column of the assembled column and the concrete is slightly damaged except for the column corner, no damage occurred in other places, and the concrete cover is intact. There is obvious necking at the joint surface of the upper and lower columns, and the failure of the specimens is in the maximum bending moment section of the column foot. The failure starts with the yield of the tensile reinforcement, which belongs to the large eccentric compression failure.

Compared with the assembled columns, the column root of the cast-in-situ concrete column is almost completely destroyed. After the destruction of the plastic hinge area develops from bottom to top, the concrete at the column foot is peeled off, the stirrup is exposed obviously, and almost all the concrete cover is peeled off. Pictures of each specimen after loading and destruction are shown in Figure 4.

3.2. Hysteresis Curve and Skeleton Curve. The hysteresis curve and the skeleton curve of the four specimens are shown in Figure 5 and 6. From the curve shape of each specimen, it can be preliminarily judged that all specimens are ductile failure modes. The shape of the hysteresis curve is full, and the skeleton curve is basically symmetrical in its origin, which can be clearly divided into the elastic stage, elastic-plastic stage, and descending stage. After the skeleton curve of each specimen reaches the peak load, there is a relatively gentle descending section, indicating that the spiral stirrup can significantly improve the ductility of the concrete column.

There is a phenomenon of "pinch" in the hysteresis curve of the assembled column, which indicates that bond-slip occurred between the column and the partial outsourcing steel pipe, and the joint can still maintain good working performance when the internal concrete is close to failure

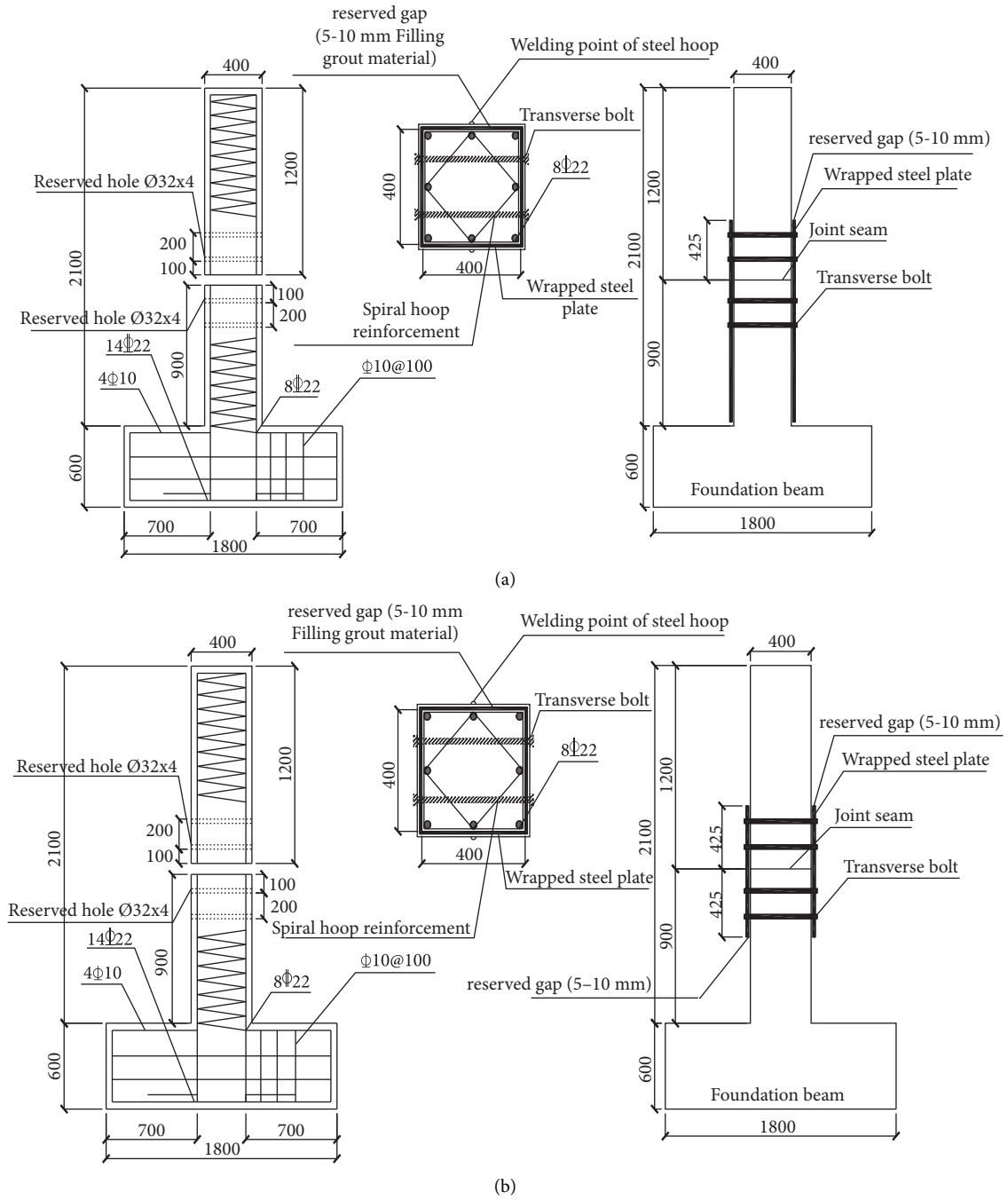


FIGURE 1: Continued.

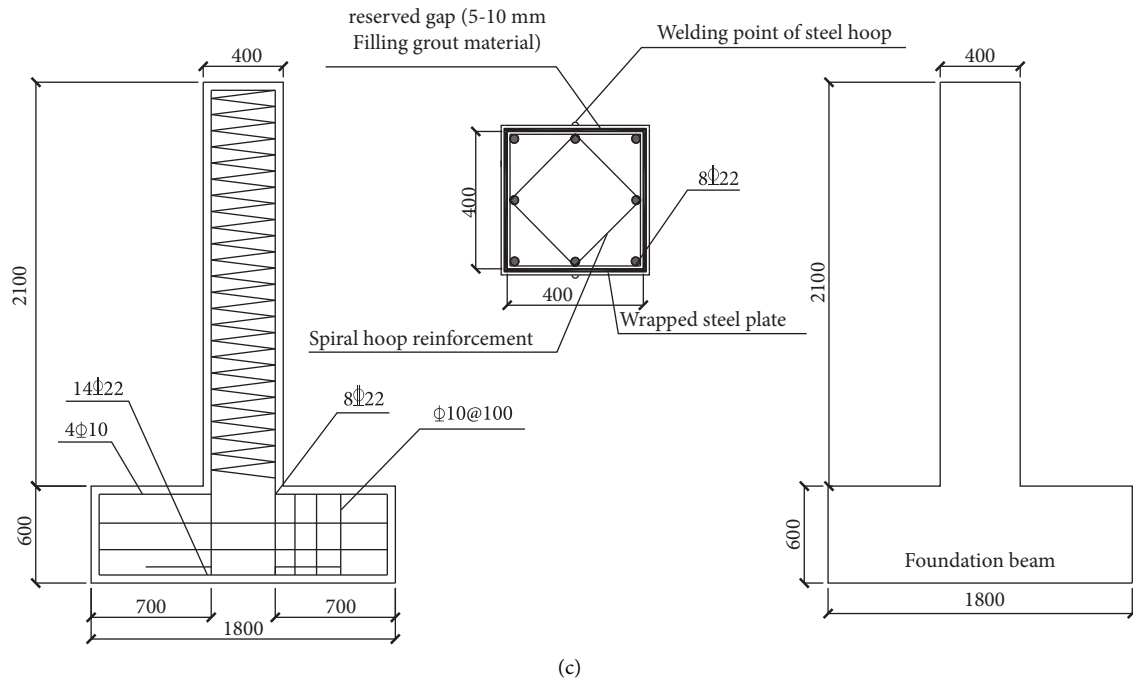


FIGURE 1: Structural details of specimens. (a) W01 and W02. (b) W03. (c) XJ-01.

due to its confinement effect. However, in the later stage of the displacement loading process, the slippage becomes larger at the larger displacement because of the weakening of the bonding force between the steel pipe and the concrete, resulting in the slight pinch phenomenon of the hysteresis curve. Under the same condition of the high axial compression ratio, the peak load of the assembled column is higher than that of the cast-in-situ column, but the bearing capacity decreases faster.

For the cast-in-situ column XJ-01, the hysteresis loop is in the shape of a shuttle, which basically coincides with the hysteresis loop of the displacement cycle, indicating that the cast-in-situ column has good seismic performance and small stiffness degradation. The stiffness degradation of specimens increases with the increase in deformation.

Through the comprehensive analysis of the hysteresis curves and the skeleton curve of the assembled columns (W01, W02, and W03), the overall shape of the assembled columns is similar to that of the cast-in-situ column XJ-01. Combined with experimental phenomena such as the maximum bending moment section, failure of all specimens appeared at the column foot and no joint failure occurred, and it can be judged that the assembled monolithic concrete column encased by partial outsourcing steel that was proposed with the high-strength spiral stirrup is safe and reliable under the low cyclic reciprocating load. The connection area of the upper and lower columns is not damaged before the member, and every assembled column and cast-in-situ column falls under bending failure, which occurs at the maximum bending moment, and the hysteretic behavior is similar to that of cast-in-place columns in actual engineering. The seismic performance of assembled columns is very similar to that of cast-in-situ

columns, and both have better seismic performance in the test.

3.3. Deformation and Ductility. Table 4 shows the main seismic performance indexes of each specimen. It can be said that the displacement ductility coefficient of all specimens is greater than 3.0, showing a good deformation capacity and meeting the requirement of the displacement ductility coefficient of the frame column which is greater than 3.0.

Under the condition of the high axial compression ratio, the ductility coefficient and ultimate drift of assembled columns are greater than those of cast-in-situ columns, which shows that the seismic capacity of the assembled column in this test is better than that of the cast-in-situ column, and the yield load and ultimate load are improved in varying degrees compared with the cast-in-situ column at the same time. The ultimate drift of all specimens is greater than 1/50, which meets the requirement of allowable ultimate deformation of the reinforced concrete frame structure under the strong earthquake action according to the Code For Seismic Design Of Buildings, and it indicates that all the specimens in this test have a great safety margin, and the seismic deformation capacity of the assembled column meets the requirements.

3.4. Influence of Outsourcing Steel Pipe Thickness on the Seismic Performance of Specimens. The thickness of the outer steel tube of the specimen W01 is 5 mm and that of the specimen W02 is 8 mm. Other structure measures are the same. The comparison of the test results between the two is shown in Figure 7.

It was found that the peak load of the specimen W02 was slightly higher than that of the specimen W01 under the high

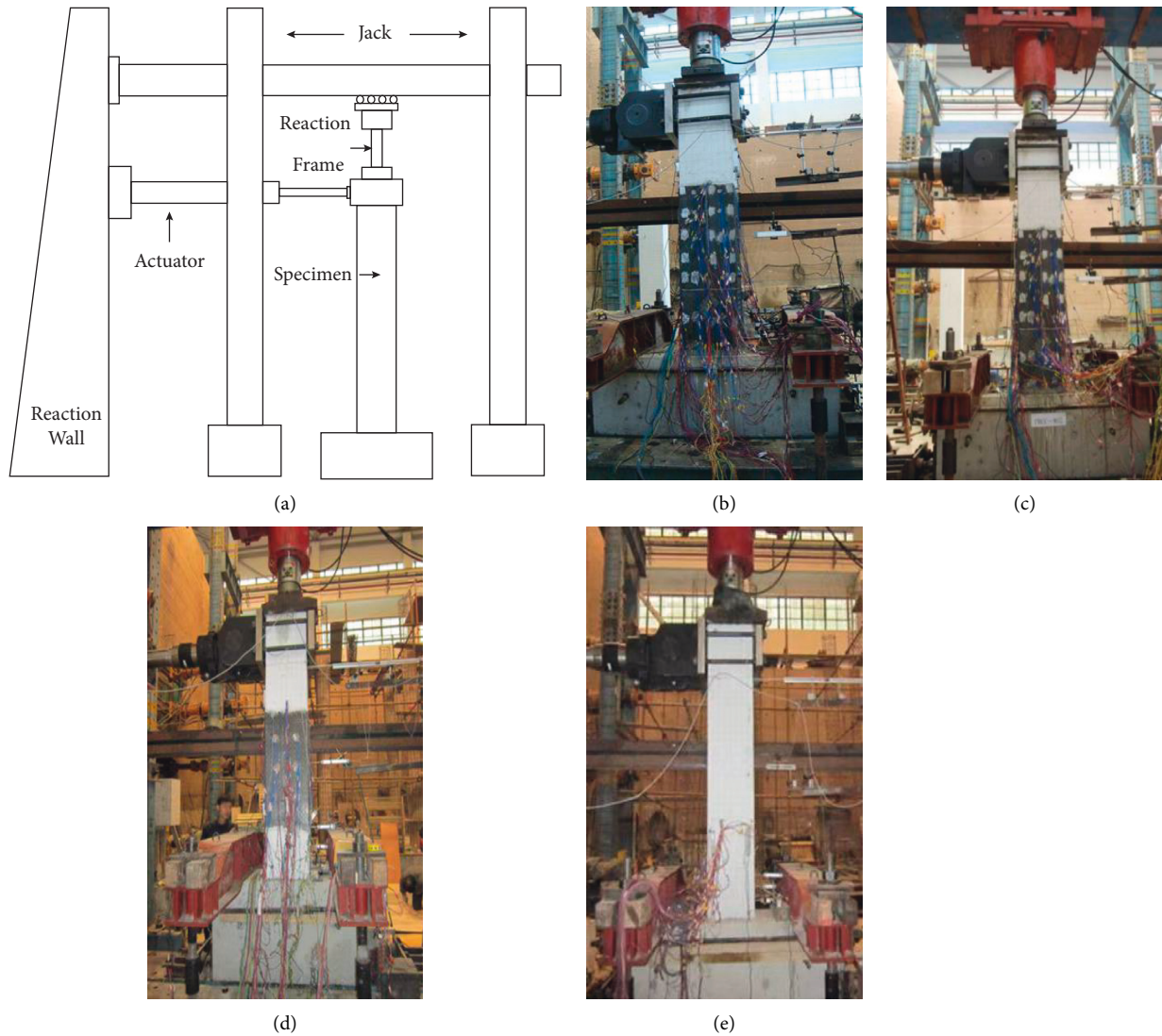


FIGURE 2: Loading device and installation and fixing of specimens. (a) Schematic diagram of the loading device. (b) W01. (c) W02. (d) W03. (e) XJ-01.

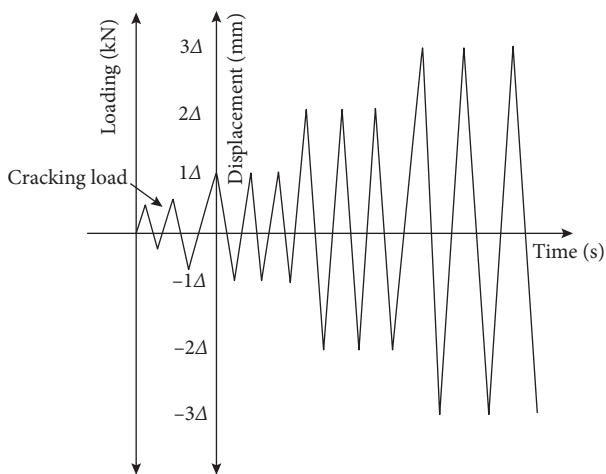


FIGURE 3: Loading system.

axial compression ratio through comparison. The decrease in the bearing capacity of the two specimens with the increasing displacement is basically synchronized.

The skeleton curves of specimens W01 and W02 are also close in the elastic stage and elastic-plastic stage, indicating that increasing the thickness of the outsourcing steel pipe does not significantly improve the hysteresis behavior of the components under the condition of meeting the bearing capacity requirements of the relevant specifications.

3.5. Comparison of the Seismic Performance between the Assembled Column and the Cast-In-Situ Column. Figure 8 shows the comparison of the hysteresis curve and the skeleton curve among specimens W01 and W03 and the cast-in-place column XJ-01.

As can be seen from the figure, the peak load of hysteresis curves of specimens W01 and W02 is similar to that of XJ-01.

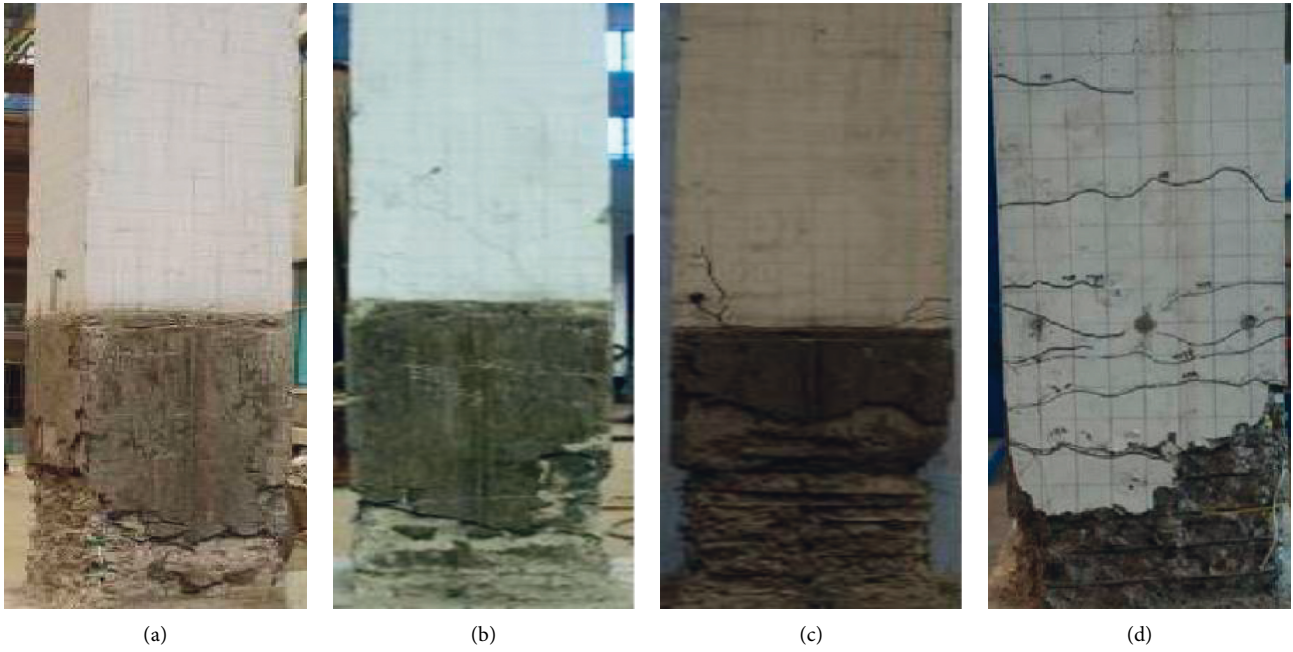


FIGURE 4: Failure form of specimens. (a) W01. (b) W02. (c) W03. (d) XJ-01.

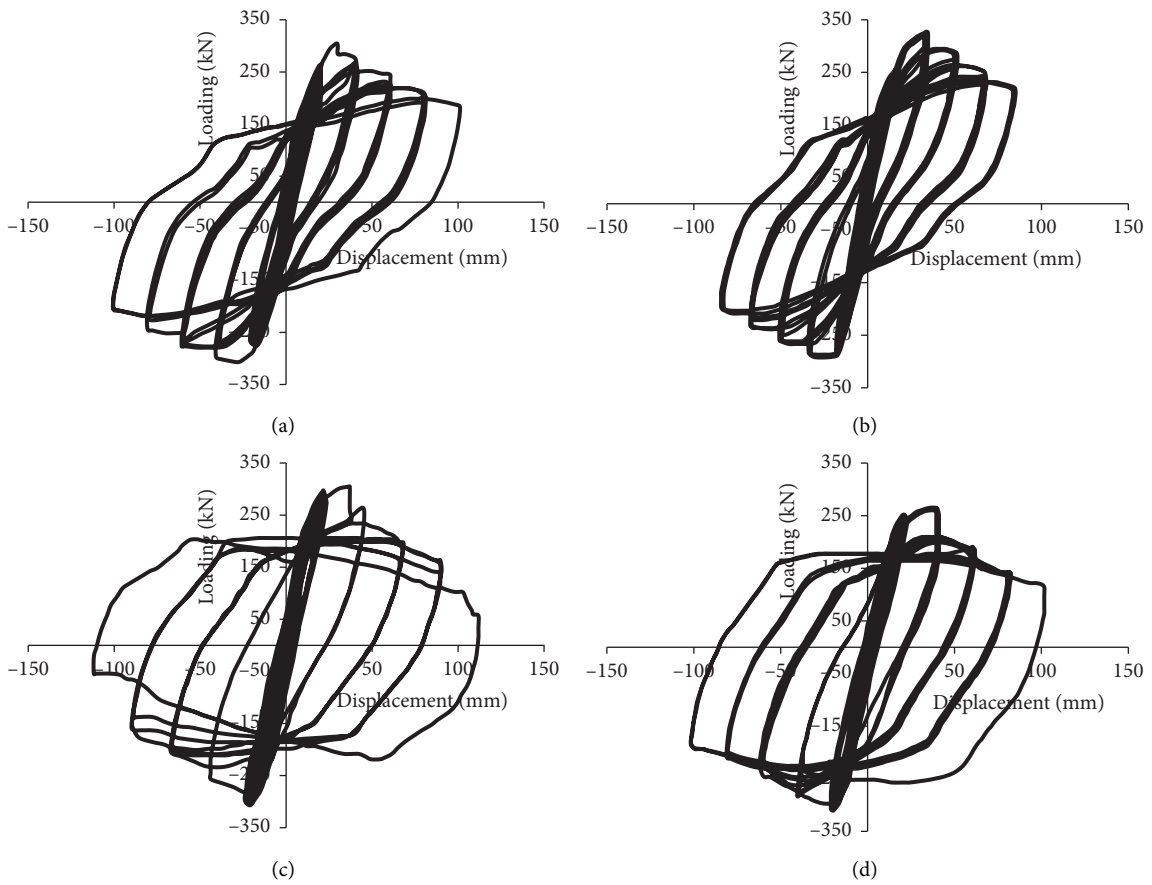


FIGURE 5: Hysteresis curves of the specimens. (a) W01. (b) W02. (c) W03. (d) XJ-01.

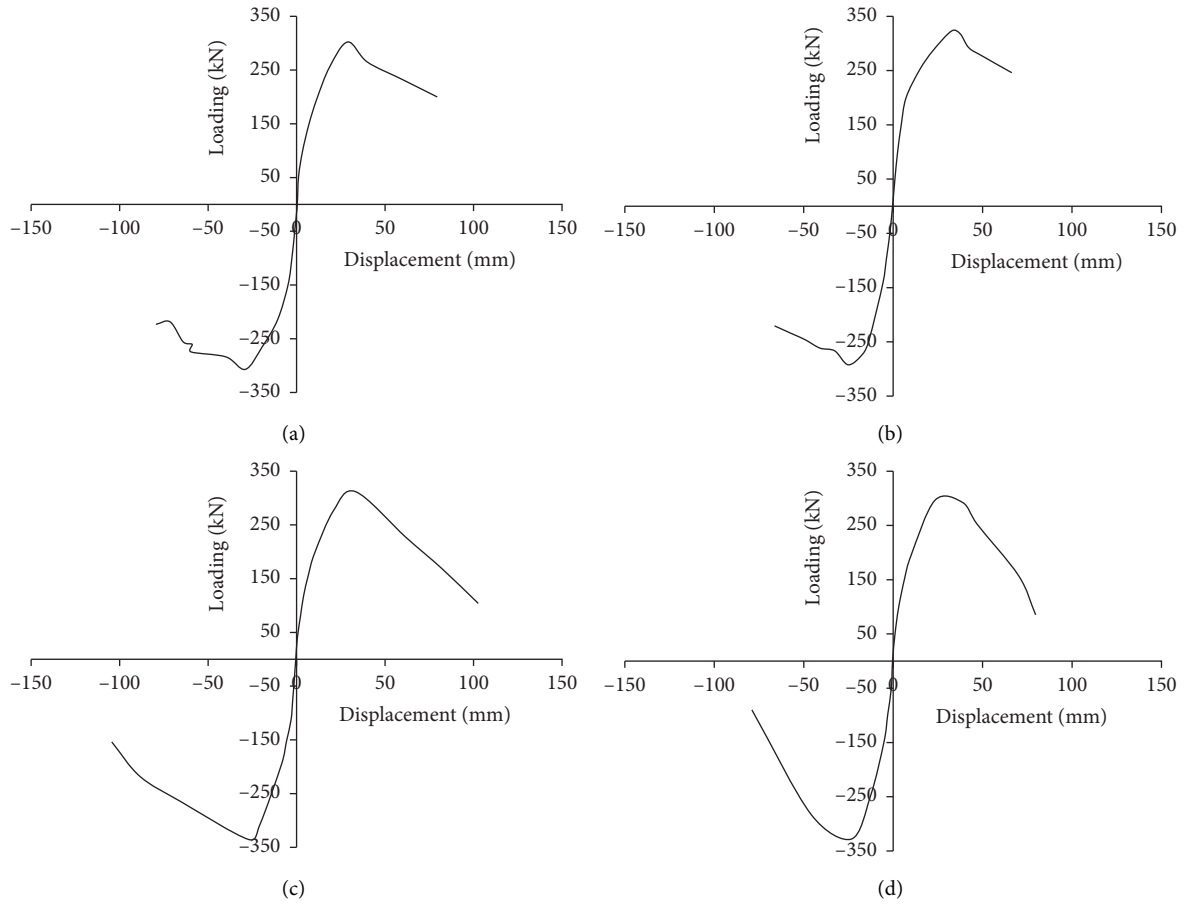


FIGURE 6: Skeleton curves of the specimens. (a) W01. (b) W02. (c) W03. (d) XJ-01.

TABLE 4: Seismic indicators of specimens.

Specimens	Ultimate load (kN)	Yield load (kN)	Yield displacement (mm)	Limiting displacement drift	Ductility factor
W01	304.69	257.447	17.068	1/30	4.23
W02	307.44	258.439	15.899	1/33	4.31
W03	304.54	258.784	14.579	1/35	3.64
XJ-01	284.62	250.340	16.527	1/40	3.50

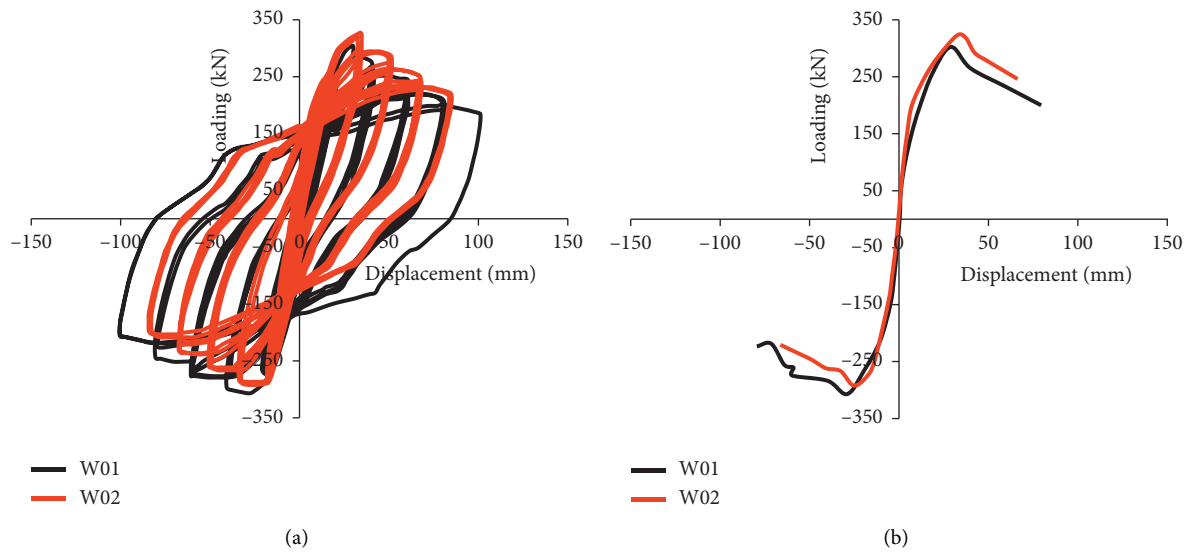


FIGURE 7: Comparison of hysteresis curves and skeleton curves of specimens with different thicknesses of outsourcing steel pipes. (a) Comparison of hysteresis curves between W01 and W02. (b) Comparison of skeleton curves between W01 and W02.

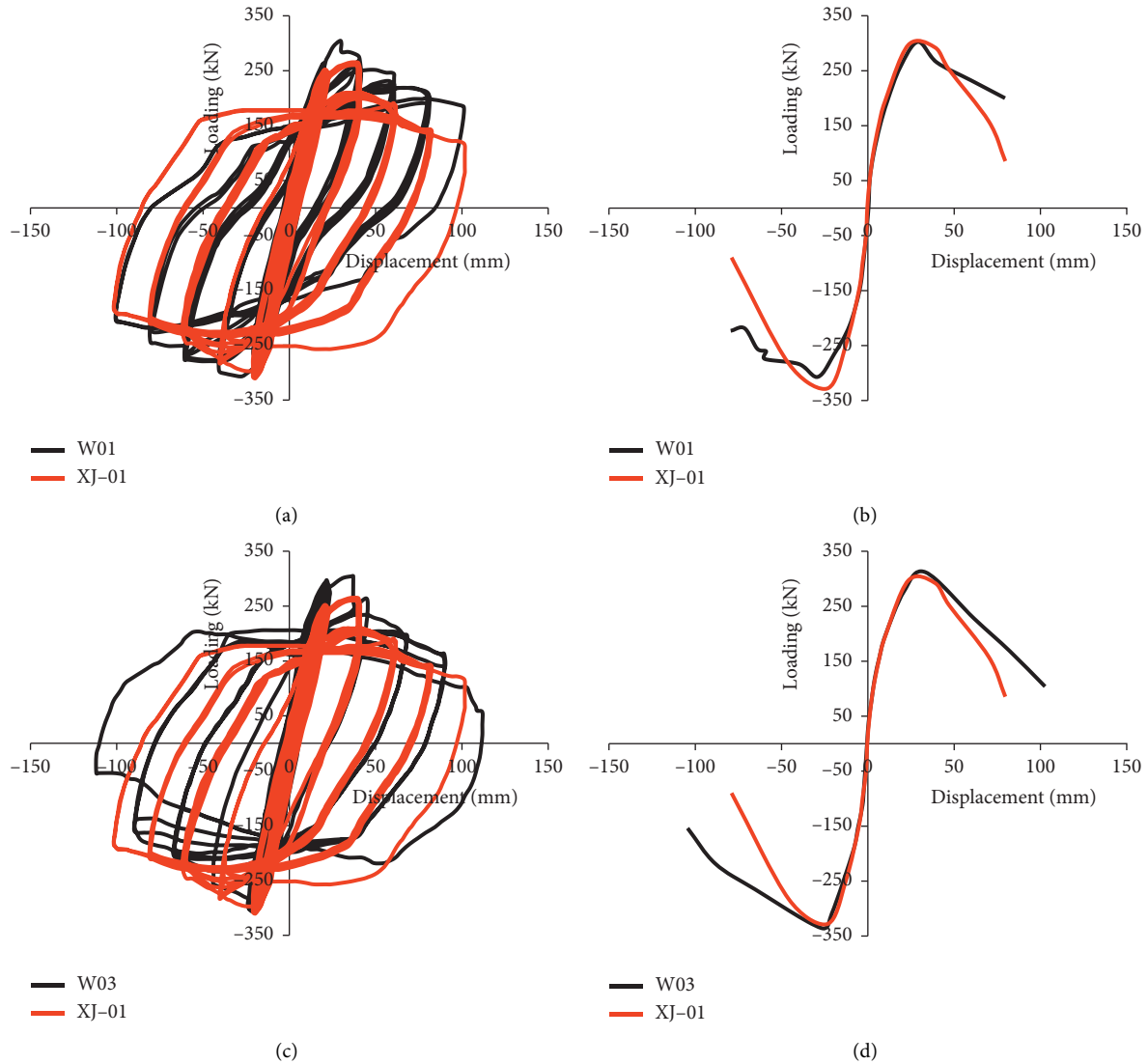


FIGURE 8: Comparison of hysteresis curves and skeleton curves of specimens with different manufacturing processes. (a) Comparison of hysteresis curves between W01 and XJ-01. (b) Comparison of skeleton curves between W01 and XJ-01. (c) Comparison of hysteresis curves between W03 and XJ-01. (d) Comparison of skeleton curves between W03 and XJ-01.

However, after reaching the peak load, the bearing capacity of W01 and W02 decreases much less with the increase of displacement than that of XJ-01. The skeleton curves of specimens W01, W02, and XJ-01 are similar in the elastic stage and elastic-plastic stage. After reaching the peak load, the strength degradation of specimens W01 and W02 is obviously slower than that of XJ-01. Under the same axial compression ratio, the assembled column has a higher bearing capacity and stronger collapse resistance at the later stage of specimen failure and under the condition of large deflection.

4. Conclusion

In this paper, the test results of four full-scale specimens under horizontal low cyclic loading such as the failure mode, hysteresis curve, and skeleton curve were studied, and the following conclusions are drawn:

- (1) The failure of the specimens occurs at the maximum bending moment section of the column foot. The failure starts with the yield of the tensile reinforcement, which belongs to large eccentric compression failure.
- (2) The hysteresis curves of all specimens are full shuttle shape with a good ductility and energy dissipation capacity.
- (3) The seismic performance of the assembled columns is basically the same as that of the cast-in-place column, while the bearing capacity, ultimate displacement, and strength degradation of the assembled column are better than those of the cast-in-situ column.
- (4) Increasing the thickness of the outer steel pipe does not significantly improve the mechanical

performance of components under the condition of meeting the bearing capacity requirements.

In conclusion, the integrity and seismic performance of the new partial outsourcing steel pipe frame column-column joint meet the requirements of the code, and it is a kind of an assembled monolithic frame column joint with a reliable connection and good seismic performance, which can provide a reference for practical engineering applications.

Data Availability

All data used in this article are true and effective, and the data that support the findings of this study are available from the corresponding author upon reasonable request.

Conflicts of Interest

The authors declare that there are no conflicts of interest regarding the publication of this paper.

Acknowledgments

This work was supported by the National Key R&D Program (grant no. 2016YFC0701100), the National Natural Science Fund (grant nos. 51678389 and 51508373), and the Tianjin Natural Science Fund Key Projects (grant no. 16JCZDJC38900).

References

- [1] Q. X. Shi, R. Chong, H. Ren, and T. Zhang, "Calculation of the compressive strength of concrete filled steel tube (CFST) based on the twin shear unified strength theory," *Chinese Quarterly of Mechanics*, vol. 36, no. 04, pp. 690–696, 2015.
- [2] Q. E. Luo, Q. P. Zhang, W. R. Cheng, Y. Wang, and Y. H. Weng, "Calculation of the compressive strength of concrete filled steel tube (CFST) based on the twin shear unified strength theory," *Industrial Construction*, vol. 38, no. 10, pp. 47–52, 2008.
- [3] Z. B. Haber, K. R. Mackie, and H. M. Al-Jelawy, "Testing and analysis of precast columns with grouted sleeve connections and shifted plastic hinging," *Journal of Bridge Engineering*, vol. 22, no. 10, Article ID 04017078, 2017.
- [4] B. Wei, *Experimental Study on Seismic Performance and Design Method of New Prefabricated Column-To-Column Connection Joints*, Xi' AN University of Architecture and Technology, Beilin, Xi'An, China, 2020.
- [5] W. H. Wei, S. Chu, L. W. Ju, and J. Zhou, "Study on seismic performance of the new-type prefabricated concrete column-column joint connected by grout-filled sleeve," *Journal of Wuhan University of Technology*, vol. 41, no. 04, pp. 40–47, 2019.
- [6] J. Y. Hu, W. K. Hong, and S. C. Park, "Experimental investigation of precast concrete based dry mechanical column-column joints for precast concrete frames," *The Structural Design of Tall and Special Buildings*, vol. 26, no. 5, pp. e1337–15, 2017.
- [7] K. Liu, J. Y. Sun, Y. S. Liu, Y. Lu, and X. J. Yang, "Experimental study on load-bearing capacity of square steel tube bolted splice joints with inner sleeve," *Journal of Building Structures*, vol. 39, no. 10, pp. 112–121, 2018.
- [8] F. X. Ding, L. Luo, L. P. Wang, S. Cheng, and Zw Yu, "Pseudo-static tests of terminal stirrup-confined concrete-filled rectangular steel tubular columns," *Journal of Constructional Steel Research*, vol. 144, pp. 135–152, 2018.
- [9] F. X. Ding, Y. C. Liu, F. Lu, D. R. Lu, and J. Chen, "Experimental study on influence of contact mode between stirrup and steel tube on seismic performance of stirrup-confined concrete-filled steel tube columns under high axial compression ratio," *Journal of Building Structures*, vol. 42, no. 09, pp. 62–72, 2021.
- [10] S. T. Liang and K. M. Li, "Experimental study of new total-prefabricated concrete frame column with dry-connection under low reverse cyclic loading," *Architectural Technology*, vol. 41, no. 01, pp. 52–55, 2010.
- [11] L. S. Lv, Z. Y. He, J. W. Xie, and Z. H. Deng, "Experimental study of a new column-column joint with assembled columns," *Concrete*, vol. 12, pp. 136–141, 2019.
- [12] J. Liu, Y. T. Xue, C. K. Wang, J. G. Nie, and Z. H. Wu, *Experimental Investigation on Seismic Performance of Mechanical Joints with Bolted Flange Plate for Precast Concrete Column*, vol. 216, Article ID 110729, 2020.
- [13] J. Li, Y. Wang, Z. Lu, and J. Li, "Experimental study and numerical simulation of a laminated reinforced concrete shear wall with a vertical seam," *Applied Sciences*, vol. 7, no. 6, pp. 629–648, 2017.
- [14] Y. Tao, S. J. Ye, and J. F. Chen, "Axial compression capacity of square steel-concrete-FRP-concrete composite columns," *Journal of Building Structures*, vol. 43, no. 03, pp. 148–158, 2022.
- [15] Q. L. Zheng, N. Wang, L. Tao, and X. Tian, "Experimental study on effects of grout defects on seismic performance of assembled concrete columns," *China Civil Engineering Journal*, vol. 51, no. 05, pp. 75–83, 2018.
- [16] X. Wang, Z. Zhang, and H. Q. He, "Experimental study on seismic behavior of assembled special-shaped column joints," *Building Structure*, vol. 50, no. 06, pp. 1–7, 2020.
- [17] Z. Gao, B. H. Wu, and T. L. Pan, "Seismic behavior of assembled single-tenon column-column joints," *Journal of Wuhan University of Technology*, vol. 41, no. 08, pp. 48–53, 2019.
- [18] Z. Lu, Z. Wang, J. Li, and B. Huang, "Studies on Seismic Performance of Precast Concrete Columns with Grouted Splice Sleeve," *Applied Sciences*, vol. 7, no. 6, pp. 571–591, 2017.
- [19] Y. T. Lv, Z. X. Guo, T. T. Huang, Y. Liu, and Y. Ye, "Experimental study on the seismic performance of earthquake-resilient prefabricated composite columns," *China Civil Engineering Journal*, vol. 53, no. 04, pp. 1–10+22, 2020.
- [20] X. L. Lv, G. J. Zhang, and S. L. Chen, "High axial compression ratio of high strength concrete frame columns in seismic performance study," *Journal of Building Structures*, vol. 30, no. 03, pp. 20–26, 2009.
- [21] *National Standard of the People's Republic of China, Standard For Test Method of concrete Structures (GB/T 50152-2012)*, China Architecture & Building Press, Beijing, China, 2014.
- [22] *National Standard of the People's Republic of China, Specification For Seismic Test of Buildings (JGJ/T 101-2015)*, China Architecture & Building Press, Beijing, China, 2015.